Structural origin of enhanced translational diffusion in two-dimensional hard-ellipse fluids

S. Davatolhagh and S. Foroozan
Department of Physics, College of Sciences, Shiraz University, Shiraz 71454, Iran
(Received 19 February 2012; published 20 June 2012)

The static correlations and diffusive dynamics of hard ellipses are investigated in the isotropic and nematic phases by Monte Carlo simulation. In particular, an enhancement of the translational diffusion with respect to the rotational diffusion is observed at an onset concentration $\phi_{\rm on}$ within the isotropic phase, which is explained in terms of the formation of unstable nematic-like regions with a mean lifetime that exceeds the characteristic time of diffusion at $\phi_{\rm on}$. The relevance to the onset of spatially heterogeneous dynamics in supercooled glass-forming liquids is discussed.

DOI: 10.1103/PhysRevE.85.061707 PACS number(s): 64.70.M−, 61.20.Lc, 64.70.kj, 66.10.cg

The diffusion of anisotropic molecules at membranes and interfaces is of immense theoretical and technological importance in biological sciences and industry. In particular, the effect of confinement between two parallel flat walls on the single-particle dynamics of anisotropic macromolecules such as ellipsoids [1], carbon nanotubes [2], and actin filaments [3] has been a subject of much experimental investigation. More recently, the diffusive dynamics of a monolayer of colloidal ellipsoids close to a flat wall has been studied systematically using the video microscopy technique [4]. In this paper, we investigate the orientational correlations and the diffusive dynamics of elongate hard ellipses in two dimensions using Monte Carlo (MC) simulations, paying particular attention to the interplay between static structure and diffusive dynamics in different phases exhibited by the system. In particular, the role played by the local fluctuations in the onset of slow relaxation dynamics characterized by an enhanced translational diffusion in comparison with the rotational diffusion within the isotropic liquid phase is discussed in detail, drawing attention to its analogies with the onset of spatially heterogeneous dynamics characteristic of fragile supercooled liquids [5,6].

For two-dimensional (2D) hard ellipses of aspect ratio $k > 4$, three different phases have been identified: isotropic, nematic, and a smectic-like solid phase [7]. The isotropic-nematic transition is believed to be continuous via a Kosterlitz-Thouless–type dislocation unbinding mechanism [8]. However, the nematic-solid transition at a higher concentration is known to be first order [7,9]. The 2D nematic phase is characterized by a vanishing order parameter in the thermodynamic limit, but a power-law decay of the corresponding correlation functions, which is generally referred to as quasi-long-range order (quasi-LRO). Such a quasi-long-range orientational order is generally expected in the 2D nematic phase [7,10] if the free energy associated with variation of orientations of molecules can be described by

$$F = \frac{1}{2}\int K(\vec{\nabla}\theta(\vec{r}))^2 d^2r, \tag{1}$$

where $\theta(\vec{r})$ is a continuous variable denoting the local molecular orientation with respect to an arbitrary fixed axis and K is an elastic constant [8,11]. As a result of Eq. (1), it can be shown that the orientational nematic order parameter

$$q \equiv \langle \cos(2\theta)\rangle \sim N^{-k_BT/2\pi K} \tag{2}$$

and the corresponding angular correlation function

$$g_2(r) \equiv \langle \cos(2[\theta(r) - \theta(0)])\rangle \sim r^{-\eta_2} \tag{3}$$

decay algebraically, where the correlation decay exponent is given by $\eta_2 = 2k_BT/\pi K$. The angular braces $\langle\cdot\rangle$ denote equilibrium ensemble average, and k_B is the Boltzmann constant. The isotropic-nematic transition is predicted to occur at a critical value of the renormalized Frank's constant given by $\pi K_c/8k_BT = 1$ [8]. It must be noted that for our athermal system of hard ellipses, the thermal energy k_BT can be considered the unit of energy. So without any loss of generality we choose $k_BT = 1$. Using the critical value of the renormalized Frank's constant $K_c = 8/\pi$, one finds the value one-fourth for the correlation decay exponent η_2 at the isotropic-nematic transition point, which is the same as that in the critical 2D Ising model. Thus, the critical area fraction ϕ_c can be ascertained using the requirement $\eta_2 = 0.25$.

Our hard ellipses are characterized by an aspect ratio $k = a/b = 9$ in order to mimic the shape of the ellipsoids used in the experiments of Ref. [4]. a and b are the semi-major and the semi-minor axes of the ellipse, respectively. The shorter length is chosen as the unit of length, thus $b = 1$, and time is measured in units of Monte Carlo steps (MCS's), which corresponds to one attempted move per particle. For our athermal hard-ellipse fluid, the area or packing fraction defined by $\phi = \pi ab\rho$ serves as the control parameter, where $\rho = N/A$ is the 2D number density and $A = 200^2$ is the area of the simulation box. A typical run consisted of 10^5 MCS's for equilibration and another 10^5 MCS's for data accumulation.

Figure 1 shows the logarithmic plot of the angular correlation function $g_2(r)$ for a range of packing fractions covering both the isotropic and the 2D nematic phases. For the largest area fractions simulated, i.e., $\phi = 0.59$ and 0.68, the curves asymptotically tend to straight lines indicating that the system possesses quasi-LRO. The least squares straight line fits into the topmost two curves give the values $\eta_2 = 0.24$ and 0.15 for the highest area fractions considered, respectively. The 2D nematic phase is characterized by decay exponents $\eta_2 \leqslant 0.25$. Thus, we conclude that the critical concentration for the isotropic-nematic transition must be $\phi_c \simeq 0.58$. This result is consistent with the previous numerical observations for ellipses of aspect ratio $k = 6$, where the 2D nematic phase was found to become stable against the dislocation unbinding mechanism only for area fractions $\phi \gtrsim 0.59$ [7]. As expected,

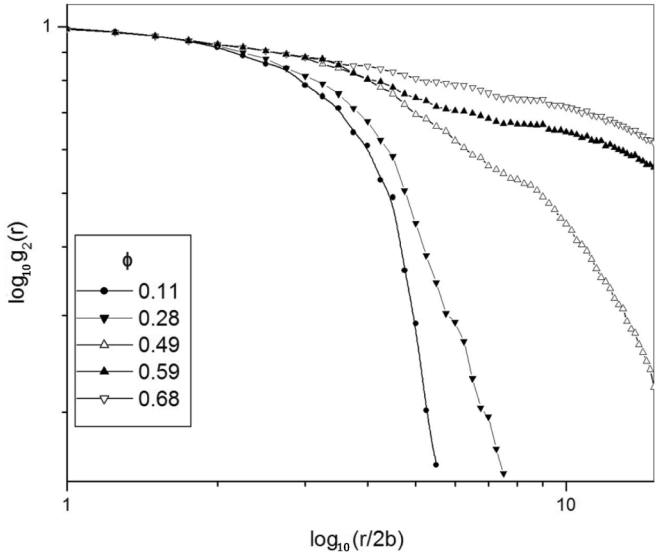

FIG. 1. The logarithmic plot of angular correlation function $g_2(r)$ for different packing fractions.

there is a weak reduction in ϕ_c with increasing the aspect ratio k [10].

The dynamic behavior of ellipses for a given degree of freedom can be characterized by the corresponding mean square displacement (MSD), which for the translational motion is defined by $\mathrm{MSD}_T = \langle \Delta r^2(t) \rangle$, where $\Delta r(t) = |\vec{r}(t) - \vec{r}(0)|$ is the displacement of a (tagged) particle during the time t. The expression for the rotational mean square displacement MSD_θ has a similar form. The subscripts T and θ denote translation and rotation, respectively. In order to obtain physically meaningful MSD's, the maximum single-particle displacements, both translation and rotation, were adjusted such that approximately 50% of the moves were accepted in the intermediate concentration range of our interest [12]. The MSD curves for the translation and rotation of the molecules are shown in Fig. 2. As can be seen from the figure, the rotational diffusion of a particle can be characterized by two diffusive time regimes, $\mathrm{MSD}_\theta \sim t^\beta$ with $\beta \approx 1$, separated by a subdiffusive region ($\beta < 1$) due to the orientational cage effect of the neighboring coordination shells, which approximately occurs at a time $t \sim \tau_\theta = (2D_\theta)^{-1}$, where τ_θ is the typical time for a substantial diffusive rotation. In the long-time regime $t \gg \tau_\theta$, the configurational changes become effective and the particle diffuses out of its "orientational" cage with the rotational motion becoming diffusive again, albeit at a slower rate in comparison with the short-time regime $t \ll \tau_\theta$ [4]. There is no discernible sign of caging in the translational diffusive motion of the molecules, shown in Fig. 2(a), which can be understood in terms of the absence of positional order beyond short range as confirmed by the pair correlation functions $g_0(r)$ (not shown) for the range of concentrations investigated. In fact, the orientational cage effect observed in Fig. 2(b) is a consequence of the medium-range orientational order that develops in the isotropic liquid on approaching the 2D nematic phase, as discussed in detail later in this paper. We did not observe any discernible orientational cage effect at low concentrations, where the orientational order is short range.

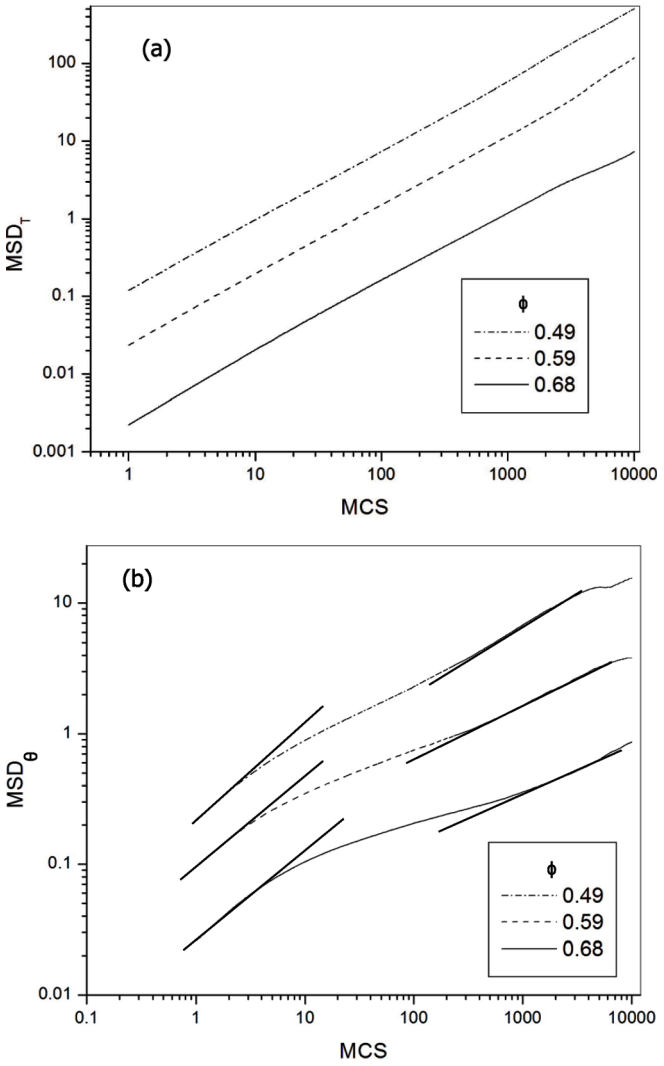

FIG. 2. The translational mean square displacement MSD_T (a) and the rotational MSD_θ (b). The solid lines in (b) are straight line fits to the short- and long-time diffusive regimes.

The diffusion coefficients are given by the slope of the corresponding MSD curves in the long-time regime. The expression for the translational diffusion is

$$D_T = \Delta \langle \Delta r^2(t) \rangle / (2d\Delta t), \tag{4}$$

where $d = 2$ is the dimension of space. The expression for rotational diffusion D_θ has the same form but with $\Delta r(t)$ replaced by $\Delta\theta(t) = |\theta(t) - \theta(0)|$. Figure 3 shows the normalized (dimensionless) translational and rotational diffusion coefficients $D_{T,\theta}(\phi)/D_{T,\theta}(0)$ as a function of the packing fraction, where $D_{T,\theta}(0)$ are the diffusion constants in the infinite dilution limit [13]. The curves are third-order polynomial fits to the data points. Clearly, the normalized D_T exceeds the normalized D_θ at a concentration that is indistinguishable from the isotropic-nematic transition point $\phi_c \simeq 0.58$, which underlines the adverse effect the quasi-long-range orientational order has on the rotational motion of the molecules. Thus, there is an intimate relation between the static structure and the diffusive dynamics of the ellipses. Furthermore, the system of elongated hard ellipses is known

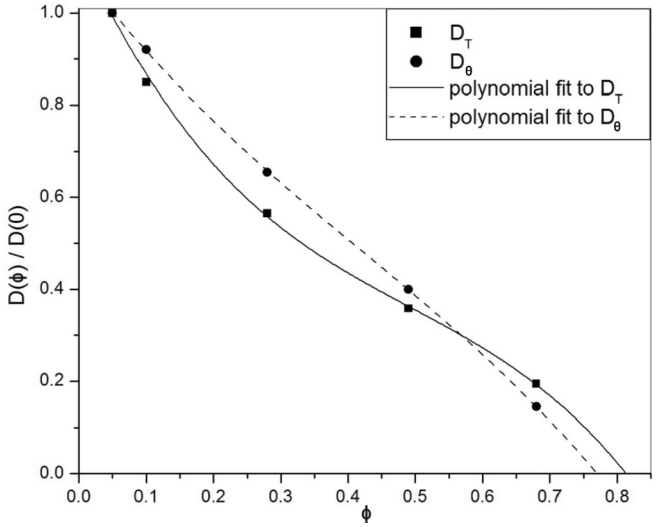

FIG. 3. The normalized translational and rotational diffusion coefficients as functions of concentration. The curves are third-order polynomial fits.

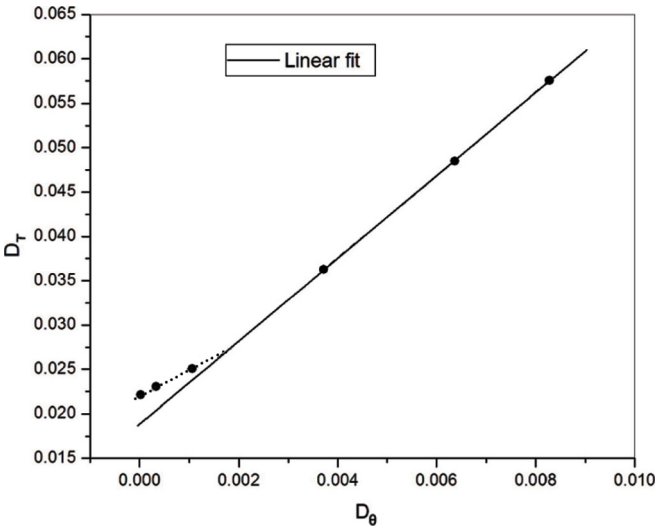

FIG. 4. The translational diffusion D_T vs the rotational diffusion D_θ. The points from top to bottom correspond to $\phi = 0.11$, 0.28, 0.35, 0.49, 0.59, and 0.68. The solid line is fit to the dilute regime. The enhancement of D_T with respect to D_θ occurs at a concentration $\phi_{\rm on} \lesssim 0.49$.

to undergo a first-order phase transition to a solid phase, characterized by long-range positional order [7]. For ellipses of aspect ratio $k = 6$, this melting point is believed to be $\phi_m \simeq 0.79$ [9]. As shown in Fig. 3, the extrapolated $D_T(\phi)/D_T(0)$, tends to vanish at an area fraction $\phi \gtrsim \phi_m$, thus underpinning the influence the long-range translational order has on the translational diffusion of the molecules. The extrapolated $D_\theta(\phi)/D_\theta(0)$, however, appears to vanish within the 2D nematic phase, thus underlining the effect the orientational order has on the rotational diffusive motion of the molecules. A further link between structure and dynamics, which is also of considerable interest for the structural glass problem, is discussed next.

Figure 4 shows a parametric plot $D_T(\phi)$ vs $D_\theta(\phi)$. It is a matter of considerable interest to note that the plot deviates from a straight line characteristic of homogeneous simple liquids at a concentration $\phi \simeq 0.48$, which signals the deviation of the transport coefficients from the Stokes-Einstein relation, characterized by an enhancement of the translational diffusion with respect to the rotational diffusion, as can be seen in Fig. 4. This "enhanced translational diffusion," or breakdown of the Stokes-Einstein relation, is also a characteristic feature of viscous liquids with heterogeneous dynamics [5,6]. In the context of fragile supercooled liquids, the heterogeneity of dynamics means that dynamics in a nanoscopic region of a deeply supercooled liquid can be orders of magnitude faster or slower than dynamics in another region just a few nanometers away [14]. Such dynamically heterogeneous regions are believed to be the main reason behind the slow relaxation dynamics, which is characterized by the stretched-exponential relaxation functions, as well as the deviation from the Stokes-Einstein relation $D_T = k_B T/6\pi\eta R^* \sim T/\eta$ of the transport coefficients, characterized by an enhancement of the translational diffusion D_T over what may be expected from the shear viscosity η ($\sim T/D_\theta$) or the rotational diffusion D_θ. The structural origin of this spatial heterogeneity of dynamics in supercooled glass-forming liquids, however, is not very clear from the experimental point of view, although it is sometimes attributed to the so-called frustration limited domains [15] that arise from competition between the energetically favored local structures (local orientational bond ordering) and the global density ordering or crystallization [16].

In the case of our hard-ellipse fluid, however, the structural origin of the dynamic heterogeneity that is reflected in the enhanced translational diffusion is easier to comprehend, which is one of its advantages, and can be assigned to the unstable nematic-like regions characterized by medium-range orientational order with a characteristic length ξ that increases rather exponentially on approaching ϕ_c [8]:

$$\xi = \xi_0 \exp(1.5\epsilon^{-1/2}). \tag{5}$$

In Eq. (5), $\epsilon = 1 - (\phi/\phi_c)$ is the reduced distance from the critical point and ξ_0 is a microscopic length scale at infinite dilution, which must be set equal to the shortest length in the system: $\xi_0 = b = 1$. However, it should be borne in mind that the diverging characteristic length ξ corresponds to the *largest* of such regions [17,18]. Indeed, the formation of nematic-like fluctuations of all sizes up to ξ is highly probable. This broadening of the distribution of sizes of the unstable nematic-like regions as $\phi \to \phi_c^-$ gives rise to a broadening of the distribution of their lifetimes t such that the bigger nematic-like regions tend to have longer lifetimes. Indeed the lifetime of the largest nematic-like regions is expected to vary as $\tau \sim \xi^z$, where the theoretical value of the dynamic exponent is $z = 2$ [19]. Thus from Eq. (5), the lifetime of the largest nematic-like regions at a given packing fraction is given by

$$\tau = \tau_0 \exp(3\epsilon^{-1/2}), \tag{6}$$

where τ_0 is a microscopic infinite dilution time scale that must be equated to the shortest time in the system, thus $\tau_0 = 1$ MCS. From Eq. (6), therefore, as ϕ increases, τ also increases with it, which leads to a broadening of the distribution of the lifetimes $(1 < t < \tau)$ for the unstable nematic-like

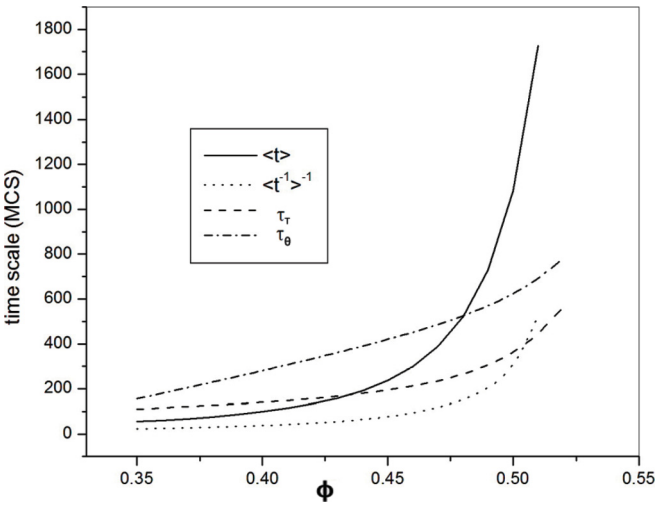

FIG. 5. A comparison of the behaviors of the four different structural and dynamical time scales as a function of concentration. The crossover point $\langle t\rangle = \tau_\theta$ at $\phi_{\rm on} = 0.48$ signals the onset of slow relaxation.

regions in the isotropic liquid. In this way, the rapidly or exponentially growing correlation time results in dynamic heterogeneity [18]. It must be noted that a similar exponential increase for the structural relaxation times characterized by the Vogel-Fulcher-Tamman equation has been found for the fragile supercooled liquids [5].

Hence the increasing τ, or more precisely the mean lifetime of the unstable nematic-like regions $\langle t\rangle$, changes the rotational behavior of the ellipses significantly as the unstable nematic-like regions are characterized by medium-range orientational order, thus resisting the rotational diffusive motion of the molecules, but having less bearing on their translational motion. The above qualitative consideration can be quantified more precisely in terms of different structural and dynamic time scales and a crossover concentration $\phi_{\rm on}$ defined by $\langle t\rangle \gtrsim (2D_\theta)^{-1}$, which signals the *onset* of slow relaxation dynamics, as follows. As shown in Fig. 4, the enhanced translational diffusion characterizing slow relaxation dynamics begins at a concentration $\phi_{\rm on} \simeq 0.48$ that is at a distance $\epsilon = 0.172$ from the 2D nematic transition. Thus, the length of the largest nematic-like regions, according to Eq. (5), is $\xi = 37$, and their lifetime is given by Eq. (6) as $\tau = \xi^2 = 1370$ MCS's. Assuming that the formation of nematic-like regions of all sizes up to ξ is equally probable [17], we can approximate the distribution of the lifetimes $G(t)$ in the range $1 < t < \tau$ by a constant and zero for $t > \tau$. Therefore, these nematic-like regions have a mean lifetime $\langle t\rangle \approx \tau^{-1}\int_1^\tau t dt = \tau/2 = 680$ MCS's at the onset concentration $\phi_{\rm on} = 0.48$. This approximate value of the mean lifetime for nematic-like regions at $\phi_{\rm on}$, can be compared with the rotational diffusion time $\tau_\theta = (2D_\theta)^{-1} = 500$ MCS's, where we have used $D_\theta = 0.001$ at $\phi_{\rm on}$, as it appears in Fig. 4. τ_θ is the typical time required for a molecule to undergo a diffusive rotation of one radian. Thus, in our system the onset concentration corresponds to the crossing of two time scales, $\langle t\rangle \gtrsim \tau_\theta$, one of structural origin, $\langle t\rangle$, and the other dynamic in nature, τ_θ. Another moment of the distribution of the lifetimes $G(t)$ that is assumed to be of some interest for the translational diffusive motion of the molecules [14,15] is $\langle t^{-1}\rangle \approx \tau^{-1}\int_1^\tau dt/t = \ln\tau/\tau$. The reciprocal of this moment has a value $\langle t^{-1}\rangle^{-1} = \tau/\ln\tau = 100$ MCS's at the onset concentration while the translational diffusion time at $\phi_{\rm on}$ is $\tau_T = ab/(2D_T) = 180$ MCS's, where we have used $ab = 9$ and $D_T = 0.025$ (Fig. 4). τ_T is the typical time required for an ellipse to translate a distance comparable to its linear size $\sqrt{ab} = 3$. Figure 5 shows the different dynamic and structural time scales as functions of the concentration, where we have used $\tau_T = 9/(2D_T)$, $\tau_\theta = (2D_\theta)^{-1}$, $\langle t\rangle = \tau/2$, and $\langle t^{-1}\rangle^{-1} = \tau/\ln\tau$. τ as a function of ϕ, is given by Eq. (6). As the figure shows for dilute systems, the mean lifetime of the nematic-like regions $\langle t\rangle$ is shorter than any of the characteristic diffusion times τ_θ and τ_T. At the crossover concentration $\phi_{\rm on} \simeq 0.48$, the mean lifetime of the nematic-like regions $\langle t\rangle$ exceeds τ_θ, as well as τ_T, at a lower concentration, and diverges at the 2D nematic transition point $\phi_c \simeq 0.58$. Therefore, the crossover point $\phi_{\rm on}$ to slow, activated, or heterogeneous dynamics, can be defined by

$$\langle t\rangle(\phi_{\rm on}) = \tau_\theta(\phi_{\rm on}). \tag{7}$$

Furthermore, Fig. 5 shows that the various time scales have very different concentration behaviors, and there is no simple relation between $\langle t\rangle$ and τ_θ, or between $\langle t^{-1}\rangle^{-1}$ and τ_T as expected in Refs. [14,15].

The result obtained here for the enhanced translational diffusion starting at an onset concentration $\phi_{\rm on}$ defined by Eq. (7) may well find direct analogy and pave the way for a better understanding of the observed dynamic heterogeneity in supercooled glass-forming liquids, based on the formation of local structures characterized by amorphous bond order that grow in linear size $\hat{\xi}$ with lowering the temperature, but lifetimes that increase rather exponentially as $\hat{\tau} \sim \exp(D\hat{\xi})$ due to the key role played by the activated processes in deeply supercooled liquids [16,18,20]. We note that an exponentially growing correlation time is also a characteristic feature of our system. Thus, we have a definition that identifies the crossover concentration (temperature) to activated transport, given by Eq. (7) and supported by numerical results of Fig. 5, which may also apply to the viscous liquids approaching their glass transition. The applicability to the fragile supercooled liquids approaching their glass transition stems from the thermodynamic theories of the structural glass transition (for a recent review, see Ref. [20]) that invoke a growing static correlation length to explain the glass transition phenomenology characterized by superArrhenius relaxation times, stretched-exponential relaxation functions, enhanced translational diffusion, and dynamic heterogeneity. However, it should be borne in mind that for our system of monodisperse ellipses, the dynamic heterogeneity in the isotropic liquid arises from unstable nematic-like regions that have geometric symmetries consistent with those in the ensuing 2D nematic phase. But in the supercooled liquids as well as monolayers of polydisperse colloidal ellipsoids that undergo a glass transition [4,21], the local structures in general have symmetries inconsistent with the ordered global phase (crystal) and cannot tile space efficiently, thus leading to geometrical frustration and glass transition.

[1] Y. Han *et al*., Science **314**, 626 (2006).
[2] R. Duggal and M. Pasquali, Phys. Rev. Lett. **96**, 246104 (2006).
[3] G. Li and J. X. Tang, Phys. Rev. E **69**, 061921 (2004).
[4] Z. Zheng and Y. Han, J. Chem. Phys. **133**, 124509 (2010).
[5] C. A. Angell *et al*., J. Appl. Phys. **88**, 3113 (2000).
[6] P. G. Debenedetti and F. H. Stillinger, Nature (London) **410**, 259 (2001).
[7] J. A. Cuesta and D. Frenkel, Phys. Rev. A **42**, 2126 (1990).
[8] J. M. Kosterlitz and D. J. Thouless, J. Phys. C **6**, 1181 (1973); J. M. Kosterlitz, *ibid*. **7**, 1046 (1974).
[9] J. Vieillard-Baron, J. Chem. Phys. **56**, 4729 (1972).
[10] M. A. Bates and D. Frenkel, J. Chem. Phys. **112**, 10034 (2000).
[11] P. G. de Gennes and J. Prost, *The Physics of Liquid Crystals*, 2nd ed. (Clarendon, Oxford, 1995).
[12] G. Rutkai and T. Kristof, J. Chem. Phys. **132**, 104107 (2010).
[13] J. M. Lahtinen, T. Hjelt, T. Ala-Nissila, and Z. Chvoj, Phy. Rev. E **64**, 021204 (2001).
[14] M. D. Ediger, Annu. Rev. Phys. Chem. **51**, 99 (2000); M. T. Cicerone and M. D. Ediger, J. Chem. Phys. **104**, 7210 (1996).
[15] G. Tarjus and D. Kivelson, J. Chem. Phys. **103**, 3071 (1995).
[16] H. Tanaka *et al*., Nat. Mater. **9**, 324 (2010); T. Kawasaki, T. Araki, and H. Tanaka, Phys. Rev. Lett. **99**, 215701 (2007).
[17] The correlation length ξ must correspond to the size of the largest clusters because of its diverging character at the critical point: the critical fluctuations cannot possibly exceed an infinite ξ. Indeed a characteristic feature of the critical point phenomena is the critical opalescence (white or milky coloration of the critical fluid) that is a consequence of the critical fluctuations of varying size that scatter visible light. The white light scattered by a critical fluid is indicative of the fact that fluctuations of all wavelengths are present with roughly the same probability.
[18] S. Davatolhagh, Eur. Phys. J. B **59**, 291 (2007); J. Phys.: Condens. Matter **17**, S1275 (2005).
[19] X. P. Qin, B. Zheng, and N. J. Zhou, J. Phys. A: Math. Theor. **44**, 345005 (2011).
[20] A. Cavagna, Phys. Rep. **476**, 51 (2009).
[21] Z. Zheng, F. Wang, and Y. Han, Phys. Rev. Lett. **107**, 065702 (2011).